Aging scaled Brownian motion

Hadiseh Safdari,[1,2] Aleksei V. Chechkin,[3,2,4] Gholamreza R. Jafari,[1] and Ralf Metzler[2,5,*]

[1]*Department of Physics, Shahid Beheshti University, G.C., Evin, Tehran 19839, Iran*

[2]*Institute of Physics & Astronomy, University of Potsdam, 14476 Potsdam-Golm, Germany*

[3]*Institute for Theoretical Physics, Kharkov Institute of Physics and Technology, Kharkov 61108, Ukraine*

[4]*Max-Planck Institute for the Physics of Complex Systems, 01187 Dresden, Germany*

[5]*Department of Physics, Tampere University of Technology, FI-33101 Tampere, Finland*

(Received 20 January 2015; published 7 April 2015)

Scaled Brownian motion (SBM) is widely used to model anomalous diffusion of passive tracers in complex and biological systems. It is a highly nonstationary process governed by the Langevin equation for Brownian motion, however, with a power-law time dependence of the noise strength. Here we study the aging properties of SBM for both unconfined and confined motion. Specifically, we derive the ensemble and time averaged mean squared displacements and analyze their behavior in the regimes of weak, intermediate, and strong aging. A very rich behavior is revealed for confined aging SBM depending on different aging times and whether the process is sub- or superdiffusive. We demonstrate that the information on the aging factorizes with respect to the lag time and exhibits a functional form that is identical to the aging behavior of scale-free continuous time random walk processes. While SBM exhibits a disparity between ensemble and time averaged observables and is thus weakly nonergodic, strong aging is shown to effect a convergence of the ensemble and time averaged mean squared displacement. Finally, we derive the density of first passage times in the semi-infinite domain that features a crossover defined by the aging time.

DOI: 10.1103/PhysRevE.91.042107 PACS number(s): 05.40.−a

I. INTRODUCTION

Deviations from normal Brownian motion were reported already in the work of Richardson on the spreading of tracers in turbulent flows [1], and quantitative deviations from the Brownian law are discussed by Freundlich and Krüger [2]. Today *anomalous diffusion* is typically defined in terms of the power-law form

$$\langle x^2(t)\rangle \sim 2K_\alpha^* t^\alpha \tag{1}$$

of the mean squared displacement (MSD) [3,4]. Depending on the value of the anomalous diffusion exponent we distinguish the regimes of subdiffusion ($0 < \alpha < 1$) and superdiffusion ($\alpha > 1$), including the special cases of Brownian motion ($\alpha = 1$) and ballistic transport ($\alpha = 2$). The generalized diffusion coefficient K_α^* in Eq. (1) has the physical dimension $\mathrm{cm}^2/\mathrm{s}^\alpha$.

Anomalous diffusion is observed in a wide range of systems, including fields as diverse as charge carrier motion in amorphous and polymeric semiconductors [5,6], dispersion of chemicals in groundwater aquifers [7], particle dispersion in colloidal glasses [8], or the motion of tracers in weakly chaotic systems [9]. With the rise of experimental techniques such as fluorescence correlation spectroscopy or advanced single particle tracking methods, the discovery of anomalous diffusion has gone through a sharp rise for the motion of endogenous and artificial tracers in living biological cells [10–15]. Concurrent to this development an increasing amount of anomalous diffusion studies is reported in artificially crowded environments mimicking aspects of the superdense state of the cellular fluid [16,17]. Within and along lipid membranes anomalous diffusion was found from experiment and simulations [18].

Brownian motion is intimately connected with the Gaussian probability density function describing the spatial spreading of a test particle as function of time. This Gaussian is effected *a forteriori* by the central limit theorem, as Brownian motion is well described on a stochastic level by the Wiener process. Anomalous diffusion loses this universal character, and instead different scenarios corresponding to the physical setting need to be considered. Among the most popular models we mention the Scher-Montroll continuous time random walk (CTRW), in which individual jumps are separated by independent, random waiting times [5,19]. If the distribution of these waiting times is scale-free, subdiffusion emerges [20]. Fractional Brownian motion and the closely related fractional Langevin equation motion are stochastic processes fueled by Gaussian yet power-law correlated noise [21,22]. Anomalous diffusion emerges when a conventional random walker is confined to move on a matrix with a fractal dimension [11,23,24]. Stochastic processes with multiplicative noise, corresponding to a space-dependent diffusion coefficient, also effect anomalous diffusion [25,26]. A contemporary summary of different anomalous diffusion processes exceeding the scope of this introduction is provided in Ref. [27].

Here we deal with the remaining of these popular anomalous diffusion models, namely scaled Brownian motion (SBM). SBM is defined in terms of the stochastic equation

$$\frac{dx(t)}{dt} = \sqrt{2\mathcal{K}(t)}\xi(t), \tag{2}$$

with nonstationary increments. The process is driven by white Gaussian noise of zero mean $\langle\xi(t)\rangle = 0$ and with autocorrelation $\langle\xi(t_1)\xi(t_2)\rangle = \delta(t_1 - t_2)$. The explicitly time dependent diffusion coefficient is taken as

$$\mathcal{K}(t) = \alpha K_\alpha^* t^{\alpha-1}. \tag{3}$$

We allow α to range in the interval (0,2), such that the process describes both subdiffusion and subballistic superdiffusion.

*rmetzler@uni-potsdam.de

The idea of a power-law time dependent diffusion coefficient is essentially dating back to Batchelor (albeit he used $\alpha = 3$) in his approach to Richardson turbulent diffusion [28]. SBM, especially in its subdiffusive form, is widely used to describe anomalous diffusion [29], albeit it is unsuitable as a physical model for systems coupled to a thermal reservoir, due to the explicit time dependence of the diffusion coefficient $\mathscr{K}(t)$. SBM was studied systematically in Refs. [26,30–32].

In stationary systems correlations measured between two times t_1 and t_2 are typically solely functions of the time difference $f(|t_1 - t_2|)$. In nonstationary systems this functional dependence is generally more involved, e.g., it can acquire the form $f(t_2/t_1)$ [33]. In such a nonstationary setting the origin of time can no longer be chosen arbitrarily. This raises the question of aging, that is, the explicit dependence of physical observables on the time span t_a between the original preparation of the system and the start of the recording of data. Traditionally, aging is considered a key property of glassy systems [34]. The aging time t_a can be adjusted deliberately in certain experiments, such as for the time of flight measurements of charge carriers in polymeric semiconductors in which the system is prepared by knocking out the charge carriers by a light flash [6]. Similarly, aging could be checked directly in blinking quantum dot systems, in which the initiation time is given by the first exposure of the quantum dot to the laser light source. In other systems, for instance, the motion of tracers in living biological cells, the aging time is not always precisely defined. In such cases it is therefore important to have cognisance of the functional effects of aging as developed here.

In the following we will analyze in detail the aging properties encoded in the SBM dynamics in both unconfined and confined settings. For free aging SBM in Sec. II we show that the result for the time averaged MSD factorizes into a term containing all the information on the aging time t_a and another capturing the physically relevant dependence on the lag time Δ. This factorization is identical to that of heterogeneous diffusion processes and scale-free, subdiffusive CTRW processes. In Sec. III we explore the aging dynamics of confined SBM. For increasing aging time t_a it is demonstrated that the nonstationary features of SBM under confinement are progressively washed out, a feature, which is important for the evaluation of measured time series. Section IV reports the first passage time density on a semi-infinite domain for aged SBM which includes a crossover between two scaling regimes as a result of the additional time scale introduced by t_a. Finally, Sec. V concludes this paper.

II. AGING EFFECT ON UNCONFINED SBM

The position autocorrelation function (covariance) for SBM in the conventional (ensemble) sense reads [30]

$$\langle x(t_1)x(t_2)\rangle = 2K_\alpha^* \min(t_1,t_2)^\alpha. \tag{4}$$

For an aged process, in which we measure the MSD starting from the aging time t_a until time t, the result for the MSD thus becomes

$$\langle x^2(t)\rangle_a = \langle [x(t_a + t) - x(t_a)]^2\rangle = 2K_\alpha^*\big[(t + t_a)^\alpha - t_a^\alpha\big]. \tag{5}$$

For a nonaged process with $t_a = 0$ the standard scaling (1) of the MSD is recovered, as it should. In the aged process, the MSD (5) is reduced by the amount accumulated until time t_a, at which the measurement starts. The limiting cases of expression (5) interestingly reveal the crossover behavior

$$\langle x^2(t)\rangle_a = \begin{cases} 2\alpha K_\alpha^* t_a^{\alpha-1} t, & t_a \gg t, \\ 2K_\alpha^* t^\alpha, & t \gg t_a. \end{cases} \tag{6}$$

While for weak aging ($t_a \ll t$) the aged MSD (5) becomes identical to the nonaged form (1), for strong aging ($t_a \gg t$) the scaling with the process time t is linear and thus, deceivingly, identical to that of normal Brownian diffusion. However, the presence of the power $t_a^{\alpha-1}$ is reminiscent of the anomaly α of the process. We note that the behavior (5) and thus (6) is identical to the result for the subdiffusive CTRW [35,36] as well as aged heterogeneous diffusion processes with a power-law form of the position dependent diffusivity [37].

In single particle tracking experiments [38–41] one measures the time series $x(t)$ of the position of a labeled particle, which is then typically evaluated in terms of the time averaged MSD. For an aged process originally initiated at $t = 0$ and measured from t_a for the duration (measurement time) t this time averaged MSD is defined in the form [36]

$$\overline{\delta_a^2(\Delta)} = \frac{1}{t - \Delta}\int_{t_a}^{t+t_a-\Delta} [x(t' + \Delta) - x(t')]^2 dt' \tag{7}$$

as a function of the lag time Δ and the aging time t_a. Averaging over an ensemble of N individual trajectories in the form

$$\left\langle \overline{\delta_a^2(\Delta)} \right\rangle = \frac{1}{N}\sum_{i=1}^{N} \overline{\delta_{a,i}^2(\Delta)}, \tag{8}$$

the structure function $\langle [x(t' + \Delta) - x(t')]^2\rangle$ in the integral of expression (7) can be evaluated in terms of the covariance (4). The exact result reads

$$\left\langle \overline{\delta_a^2(\Delta)} \right\rangle = \frac{2K_\alpha^*}{(\alpha+1)(t-\Delta)}\big[(t + t_a)^{\alpha+1} - (t_a + \Delta)^{\alpha+1} - (t + t_a - \Delta)^{\alpha+1} + t_a^{\alpha+1}\big]. \tag{9}$$

In the absence of aging, we recover the known result [26,31,32]

$$\left\langle \overline{\delta^2(\Delta)} \right\rangle \sim 2K_\alpha^* \frac{\Delta}{t^{1-\alpha}}. \tag{10}$$

Its linear lag time dependence contrasts the power-law form of the ensemble averaged MSD (1) and thus demonstrates that this process is weakly nonergodic in the sense of the disparity [27,42,43]

$$\left\langle \overline{\delta^2(\Delta)} \right\rangle \neq \langle x^2(\Delta)\rangle. \tag{11}$$

The equivalence and therefore ergodicity in the Boltzmann sense is only restored in the Brownian case $\alpha = 1$. In the presence of aging, expansion of expression (9) in the limit $t, t_a \gg \Delta$ of short lag times yields

$$\left\langle \overline{\delta_a^2(\Delta)} \right\rangle \sim \Lambda_\alpha(t_a/t)\left\langle \overline{\delta^2(\Delta)} \right\rangle, \tag{12}$$

in which we defined the so-called aging depression as

$$\Lambda_\alpha(z) = (1 + z)^\alpha - z^\alpha. \tag{13}$$

In this experimentally relevant limit all the information on the age of the process is thus contained in the aging depression Λ_α, and the physically important dependence on the lag time Δ factorizes, such that Eq. (12) contains the nonaged form (10). Result (12) is identical to the behavior of aged subdiffusive CTRW [36] and heterogeneous diffusion processes [25]. In the limit $t_a \gg t$ of strong aging, the time averaged MSD (9) remarkably reduces to the form

$$\left\langle \overline{\delta_a^2(\Delta)} \right\rangle = 2\alpha K_\alpha^* t_a^{\alpha-1} \Delta. \tag{14}$$

In this limit the time averaged MSD thus becomes equivalent to the aged ensemble averaged MSD, $\langle \overline{\delta_a^2(\Delta)} \rangle = \langle x^2(\Delta) \rangle_a$, as evidenced by comparison with result (5). In this limit, that is, ergodicity is apparently restored, as already observed for aged CTRW processes [36].

Figure 1 shows the behavior of the ensemble and time averaged MSD for unconfined SBM at different aging times in the subdiffusive case with $\alpha = 1/2$. The thin lines depict the simulations results for the time averaged MSD for 20 individual trajectories. The first observation is that the amplitude spread between these 20 time traces is fairly small. Note that the larger scatter for longer lag times Δ is due to worsening statistics when Δ approaches the trace length t. The circles in Fig. 1 correspond to the average over the 20 different results for the time averaged MSD. The latter compare very nicely with the theoretical expectation (12). Finally, the thick green line is the theoretical result (5) for the ensemble averaged MSD. The detailed behavior in the three different aging regimes is as follows:

(i) In the nonaged case ($t_a = 0$, top panel of Fig. 1) the power-law growth $\langle x^2(t) \rangle \simeq t^\alpha$ of the MSD contrasts the linear form $\langle \overline{\delta^2(\Delta)} \rangle \simeq \Delta$, this disparity being at the heart of the weak ergodicity breaking [26,31,32].

(ii) In the weak aging case ($t_a = 10^3$, middle panel of Fig. 1) a major change is visible in the behavior of the MSD, namely, we see the crossover from the aging-dominated linear scaling $\langle x^2(t) \rangle \simeq t_a^{\alpha-1} t$ to the anomalous scaling $\langle x^2(t) \rangle \simeq t^\alpha$, encoded in Eqs. (6). The behavior of the time averaged MSD is largely unchanged in comparison to case (i).

(iii) In the strong aging case ($t_a = 10^6$, bottom panel of Fig. 1) we see the apparent restoration of ergodicity: ensemble and time averaged MSDs coincide, as given by Eq. (14).

The convergence of the ensemble and time averaged MSDs in the strong aging case for the superdiffusive case with $\alpha = 3/2$ is nicely corroborated in Fig. 2.

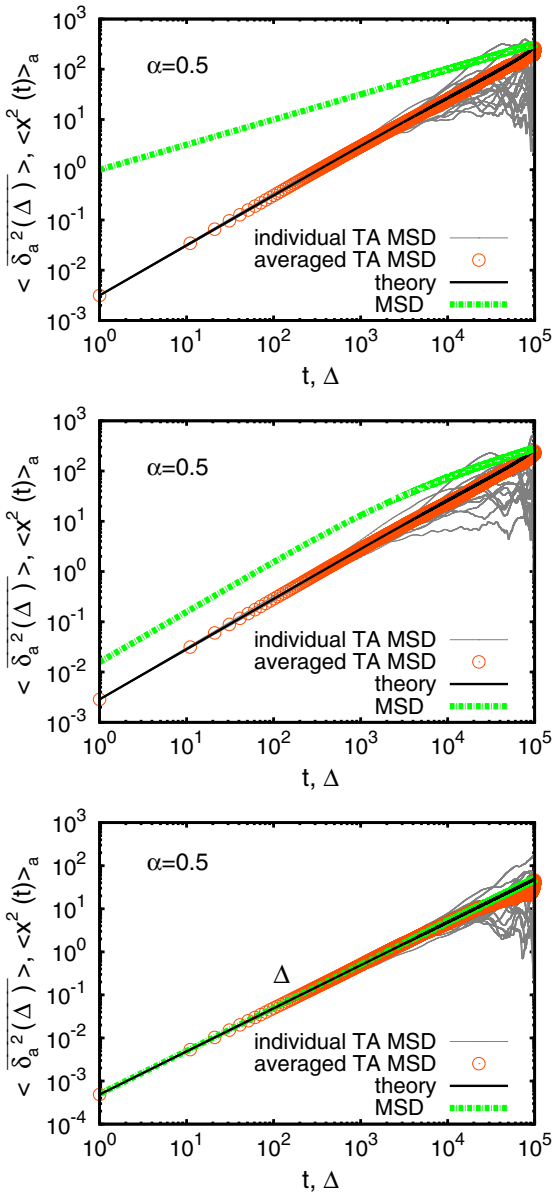

FIG. 1. (Color online) Ensemble and time averaged MSD for SBM with $\alpha = 1/2$. Thin lines: Time averaged MSD for 20 individual trajectories from simulations of the SBM Langevin equation (2) with trajectory length $t = 10^5$. Circles: Averages over those 20 trajectories. Black thin line: Theory result (12). Thick green line: Ensemble averaged MSD (5). Three different aging times were considered (top to bottom): (a) nonaged case $t_a = 0$, (b) weak aging case $t_a = 10^3$, and (c) strong aging case $t_a = 10^6$. In all simulations $K_\alpha^* = 1/2$ in the following, unless otherwise indicated.

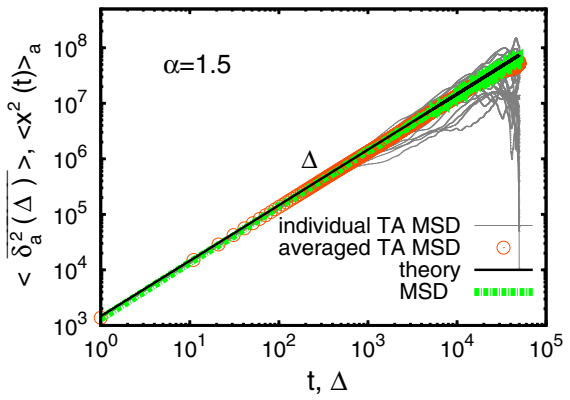

FIG. 2. (Color online) Ensemble and time averaged MSD for SBM (2) with $\alpha = 3/2$ in the strong aging case, $t_a = 10^6$. The observation time is $t = 10^5$. The spread of the 20 single trajectory time averages is fairly small. As before, the ensemble and time averaged MSDs coincide, apparently restoring ergodicity.

III. AGING EFFECT ON CONFINED SBM

In many cases an observed particle cannot be considered free during the observation. Examples contain particles moving in confined space, for instance, within the confines of living biological cells [14,44]. Similarly, particles measured in optical tweezer setups experience a confining Hookean force [12,17,45]. As a generic example for confined SBM we consider the linear restoring force $-kx(t)$ with force constant k. The corresponding stochastic equation for this confined SBM reads [32]

$$\frac{dx(t)}{dt} = -kx(t) + \sqrt{2\alpha K_\alpha^* t^{(\alpha-1)}}\xi(t), \tag{15}$$

where, as before, $\xi(t)$ represents white Gaussian noise of zero mean. The covariance in the confined case yields in the form [32]

$$\langle x(t_1)x(t_2)\rangle = 2K_\alpha^* t_1^\alpha e^{-k(t_1+t_2)} M(\alpha,\alpha+1,2kt_1), \tag{16}$$

for $t_1 < t_2$ in terms of the confluent hypergeometric function of the first kind, also referred to as the Kummer function [32,46]. Based on this result we now present the ensemble and time averaged MSDs.

A. Ensemble averaged MSD of confined SBM

The ensemble averaged MSD for aging SBM, $\langle x^2(t)\rangle_a = \langle [x(t_a+t)-x(t_a)]^2\rangle$ becomes

$$\langle x^2(t)\rangle_a = 2\mathscr{M}_1(t_a+t) + 2\mathscr{M}_1(t_a) - 4e^{-kt}\mathscr{M}_1(t_a), \tag{17}$$

where we used the abbreviation

$$\mathscr{M}_1(t) = K_\alpha^* t^\alpha \exp(-2kt) M(\alpha,\alpha+1,2kt). \tag{18}$$

In the limit $k \to 0$ of vanishing confinement, Eq. (5) for free SBM is readily recovered from the property $M(\alpha,\alpha+1,0) = 1$.

We now discuss the result (17) in the three limits of the nonaged, weakly aged, and strongly aged processes. The analysis reveals a rich behavior depending on the values of the aging time t_a and the anomalous diffusion exponent α. For sub- and superdiffusion, respectively, the various crossovers are displayed in Figs. 3 and 4.

(i) In the absence of aging ($t_a = 0$) we get back to the result

$$\langle x^2(t)\rangle = 2\mathscr{M}_1(t) \tag{19}$$

reported in Ref. [32]. For $t \ll 1/k$ this reduces to the nonaged free SBM result (1), while in the long time limit $t \gg 1/k$ we use the expansion

$$M(\alpha,\alpha+1,z) \sim \alpha\frac{\exp(z)}{z} \tag{20}$$

of the Kummer function to obtain [32]

$$\langle x^2(t)\rangle \sim \frac{\alpha K_\alpha^*}{k} t^{\alpha-1}. \tag{21}$$

This result underlines the inherently nonstationary character of SBM: for subdiffusion the MSD $\langle x(t)^2\rangle$ progressively decays, while for superdiffusion it increases. This property reflects the time dependence of the temperature encoded in the diffusivity (3) [32]. This nonaged behavior is shown in Figs. 3 and 4 as the gray lines for two different strengths k of the external confining potential. How does aging modify this behavior?

(ii) We first consider the case $t_a \ll 1/k$. If in addition $t \ll 1/k$, this is but the above result (5) for free aging SBM. However, care needs to be taken when $t \gg 1/k$. From Eq. (17) we find that the first two terms (the third one is exponentially

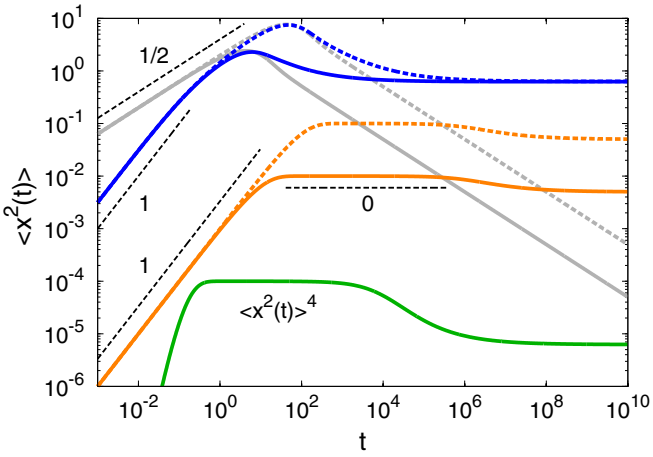

FIG. 3. (Color online) Ensemble averaged MSD $\langle x^2(t)\rangle$ for confined aging SBM in the subdiffusive case with $\alpha = 0.5$ and $K_\alpha = 1$ at different aging times: (i) nonaged ($t_a = 0$) denoted by the gray lines; (ii) weakly aged ($t_a = 0.1$) denoted by the blue lines; and (iii) strongly aged ($t_a = 10^6$) denoted by the orange lines. In all cases, the full lines correspond to the force constant $k = 0.1$, while the dashed lines stand for $k = 0.01$. The green line at the bottom of the graph is a blowup [$\langle x^2(t)\rangle^4$ of the case $t_a = 10^6$ and $k = 0.1$] in which the crossover between the two plateaux is more visible.

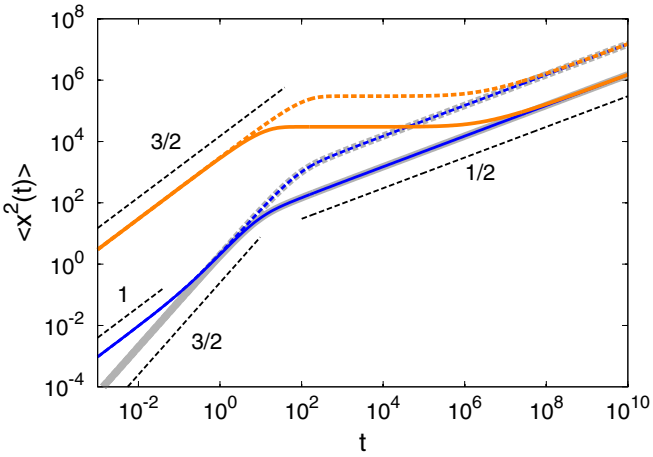

FIG. 4. (Color online) Ensemble averaged MSD $\langle x^2(t)\rangle$ for confined aging SBM in the superdiffusive case with $\alpha = 1.5$ and $K_\alpha = 1$ at different aging times: (i) nonaged ($t_a = 0$) denoted by the gray lines; (ii) weakly aged ($t_a = 0.1$) denoted by the blue lines; and (iii) strongly aged ($t_a = 10^6$) denoted by the orange lines. In all cases, the full lines correspond to the force constant $k = 0.1$, while the dashed lines stand for $k = 0.01$. In all cases the terminal scaling $\simeq t^{\alpha-1}$ is reached.

small in t and can be neglected) lead to the asymptotic behavior

$$\langle x^2(t)\rangle_a \sim \frac{\alpha K_\alpha^*}{k} t^{\alpha-1} + 2K_\alpha^* t_a^\alpha. \quad (22)$$

This implies that for subdiffusion ($0 < \alpha < 1$) the first term tends to zero and the leading behavior is the plateau

$$\langle x^2(t)\rangle_a \sim 2K_\alpha^* t_a^\alpha. \quad (23)$$

Even for very weak aging, the ensemble averaged MSD $\langle x^2(t)\rangle_a$ becomes t_a dependent. When experimental data are evaluated and the exact equivalence $t_a = 0$ is not guaranteed, the erroneous conclusion could be drawn that the process is stationary. Note, however, that result (23) is independent of the strength k of the confining potential and only depends on the diffusion coefficient K_α^* and the aging time t_a, mirroring the fact that this term stems from the initial free motion during the aging period and thus indicates an out-of-equilibrium behavior. Conversely, for superdiffusion ($\alpha > 1$) the leading order term indeed shows the growth

$$\langle x^2(t)\rangle_a \sim \frac{\alpha K_\alpha^*}{k} t^{\alpha-1} \quad (24)$$

of the ensemble averaged MSD. The weakly aged behavior is shown in Figs. 3 and 4 as the blue lines.

(iii) With the asymptotic expansion (20) of the Kummer function, we find that in the strong aging regime $t_a \gg 1/k$ the ensemble averaged MSD becomes

$$\langle x^2(t)\rangle_a \sim \alpha k^{-1} K_\alpha^* \left[(t_a + t)^{\alpha-1} + t_a^{\alpha-1}(1 - 2e^{-kt})\right]. \quad (25)$$

At short times $t \ll 1/k$, this leads us back to the unconfined result $\langle x^2(t)\rangle_a \sim 2\alpha K_\alpha^* t_a^{\alpha-1} t$ of Eq. (6). At long time $t \gg 1/k$, however, we have to distinguish two different regimes. First, for $t_a \gg t \gg 1/k$ we obtain the plateau

$$\langle x^2(t)\rangle_a \sim \frac{2\alpha K_\alpha^*}{k} t_a^{\alpha-1}, \quad (26)$$

which differs from the above result (24) by the factor of 2. Second, for $t \gg t_a \gg 1/k$ the leading order according to Eq. (25) again differs between sub- and superdiffusive motion. For $0 < \alpha < 1$ the plateau

$$\langle x^2(t)\rangle_a \sim \frac{\alpha K_\alpha^*}{k} t_a^{\alpha-1} \quad (27)$$

emerges. Note, however, that in comparison to Eq. (26) we now have half the amplitude. In the superdiffusive case $\alpha > 1$ we recover result (24). This intricate behavior is shown in Figs. 3 and 4 as the orange lines. In Fig. 3 we pronounce the crossover between the two plateaux by plotting the fourth power of the ensemble MSD as the green line.

B. Time averaged MSD of confined SBM

The time averaged MSD for confined SBM can be derived by substituting the above covariance (16) into the integral (7). By help of the relation [47]

$$\int^x y^\alpha e^{-y} M(\alpha, 1+\alpha, y)\, dy = \frac{1}{1+\alpha} x^{1+\alpha} e^{-x} M(1+\alpha, 2+\alpha, x), \quad (28)$$

this procedure yields the general result

$$\left\langle \overline{\delta_a^2(\Delta)} \right\rangle = \frac{2K_\alpha^*}{(t-\Delta)(1+\alpha)} \{\mathscr{M}_2(t+t_a) - \mathscr{M}_2(t_a+\Delta) + \mathscr{M}_2(t+t_a-\Delta) - \mathscr{M}_2(t_a) - 2e^{-k\Delta}\left[\mathscr{M}_2(t+t_a-\Delta) - \mathscr{M}_2(t_a)\right]\}, \quad (29)$$

where we used the abbreviation

$$\mathscr{M}_2(t) = t^{1+\alpha} e^{-2kt} M(1+\alpha, 2+\alpha, 2kt). \quad (30)$$

(i) In the limit $k \to 0$ we recover the result (9) of unconfined aging SBM, while the complete absence of aging restores the result from Ref. [32].

In the presence of confinement, we distinguish the following regimes:

(ii) We now consider the case when the aging time is short compared to the relaxation time of the system, $t_a \ll 1/k$. From the general expression (29) we then find the following behaviors: (a) when in addition the lag time is short ($t \gg 1/k \gg \Delta \gtrsim t_a$) we recover the nonaged result (10) with its linear scaling in the lag time Δ. (b) When the lag time is long ($t \gg \Delta \gg 1/k \gg t_a$) we find the plateau

$$\left\langle \overline{\delta_a^2(\Delta)} \right\rangle \sim \frac{2K_\alpha^*}{k} t^{\alpha-1} \quad (31)$$

known from the nonaged case [27]. (c) Finally, when the lag time approaches the length t of the time series, the time averaged MSD

$$\left\langle \overline{\delta_a^2(\Delta)} \right\rangle \sim \frac{\alpha K_\alpha^*}{k} t^{\alpha-1} \quad (32)$$

becomes equivalent to the ensemble averaged MSD, Eq. (24). In contrast to the ensemble averaged MSD, we thus find that the time averaged MSD is not affected by short aging times as compared to the relaxation time scale $t_a \ll 1/k$.

(iii) The second, more interesting case corresponds to long aging times compared to the relaxation time scale $t_a \gg 1/k$. When also $t \gg 1/k$, the result is independent of the specific magnitude of the lag time. From the general expression (29) by help of relation (20) we obtain

$$\left\langle \overline{\delta_a^2(\Delta)} \right\rangle \sim \frac{K_\alpha^*}{k(t-\Delta)} \left\{(t+t_a)^\alpha - (\Delta+t_a)^\alpha + (1-2e^{-k\Delta})\left[(t+t_a-\Delta)^\alpha - t_a^\alpha\right]\right\}. \quad (33)$$

If we now consider the regime in which the lag time is short, $t, t_a \gg 1/k \gg \Delta$, we obtain result (12) with the aging depression (13) from unconfined aging SBM. In the opposite limit $t, t_a \gg \Delta \gg 1/k$ when the lag time is long compared to the relaxation time, we find

$$\left\langle \overline{\delta_a^2(\Delta)} \right\rangle \sim \Lambda_\alpha(t_a/t) \left\langle \overline{\delta^2(\Delta)} \right\rangle, \quad (34)$$

where $\langle \overline{\delta^2(\Delta)} \rangle$ is equal to expression (31) and $\Lambda_\alpha(z)$ is again the aging depression (13). In the strong aging limit $t, t_a \gg \Delta \gg 1/k$, that is, the aged time averaged MSD is generally given by $\langle \overline{\delta_a^2(\Delta)} \rangle \sim \Lambda_\alpha(t_a/t) \langle \overline{\delta^2(\Delta)} \rangle$ for any lag time. Similar to subdiffusive CTRW processes [36], the occurrence of the factor Λ_α appears like a general feature for the aging dynamics of SBM.

Figure 5 shows the behavior of the ensemble and time averaged MSD for confined SBM at different degrees of

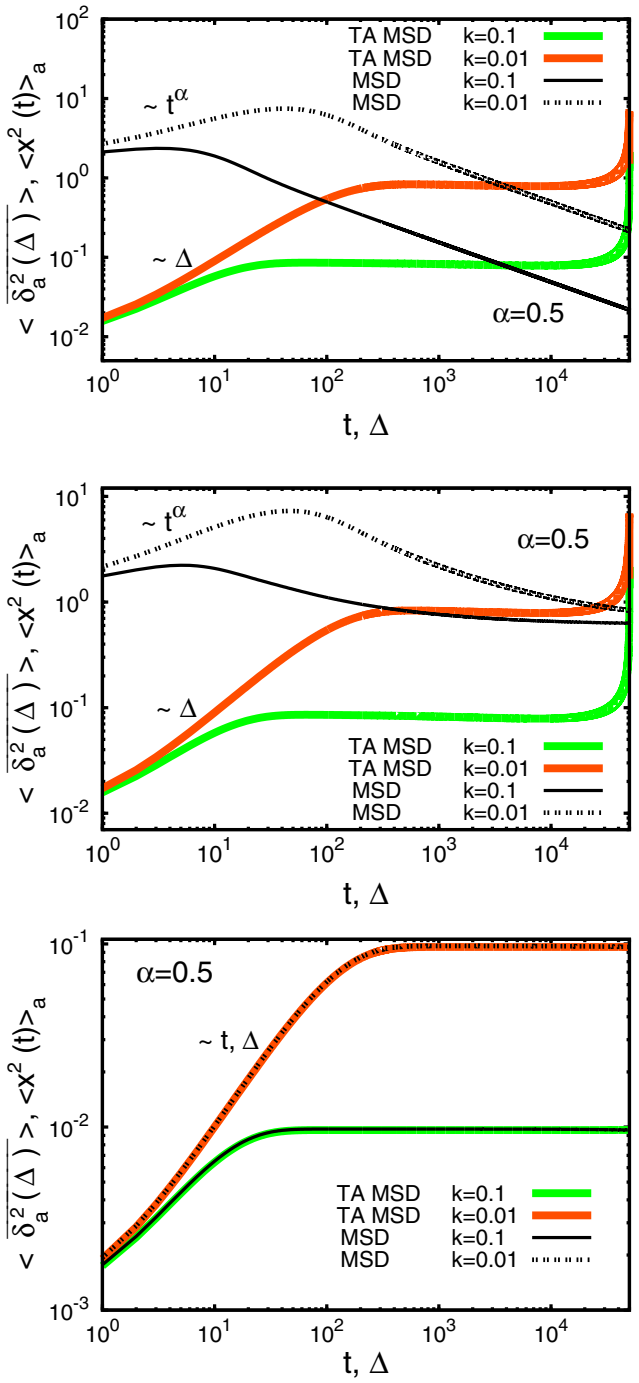

FIG. 5. (Color online) Ensemble and time averaged MSD for confined SBM for $\alpha = 1/2$. From top to bottom, the panels represent the nonaged ($t_a = 0$) case, the case of weak aging ($t_a = 10^{-1}$), and the case of strong aging ($t_a = 10^6$), where the observation time is chosen as $t = 5 \times 10^4$. The lines represent Eqs. (17) and (29). The force constants k are indicated in the panels. Note that the time averaged MSD indeed converges to the ensemble MSD in the limit $\Delta \to t$, compare the discussion in Ref. [32] and the zoom-in provided in Fig. 7.

aging. The graphs represent the full behavior according to Eqs. (17) and (29). In the absence of aging, the initial linear growth $\langle \overline{\delta_a^2(\Delta)} \rangle \simeq \Delta$ of the time averaged MSD crosses over to an apparent plateau, contrasting the functional behavior

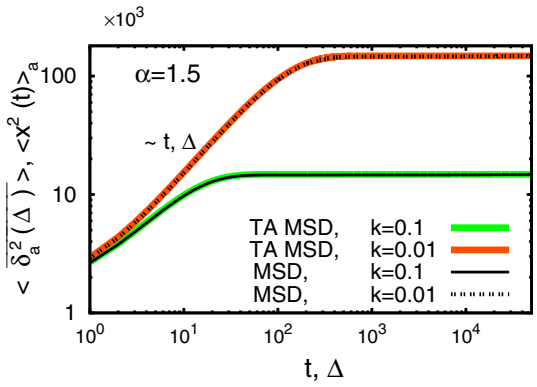

FIG. 6. (Color online) Ensemble and time averaged MSD for confined SBM with $\alpha = 3/2$ in the strong aging case with $t_a = 10^6$. The observation time is $t = 5 \times 10^4$.

of the ensemble average: at short times we observe the power-law growth $\langle x^2(t) \rangle_a \simeq t^\alpha$ of unconfined SBM, while after engaging with the confining potential, the monotonic decrease $\langle x^2(t) \rangle_a \simeq t^{\alpha-1}$ reflects the temporal decay of the noise strength (i.e., the temperature) [32]. When aging effects come into play, the ensemble averaged MSD displays notable differences. In the case of weak aging displayed in the middle panel of Fig. 5 deviations from the power-law decay of $\langle x^2(t) \rangle_a$ become apparent for longer times $t \gg t_a \gg 1/k$. Eventually the convergence to a common value independent of the force constants is observed, as predicted by Eq. (23). Finally, in the strong aging limit, the ensemble and time averaged MSD are equivalent and ergodicity is seemingly restored: $\langle \overline{\delta_a^2(\Delta)} \rangle = \langle x^2(\Delta) \rangle_a$, as can be witnessed in the bottom panel of Fig. 5. The apparent equivalence of ensemble and time averaged MSDs in the strong aging limit is also proven in the superdiffusive case for $\alpha = 3/2$ in Fig. 6. The slight discrepancy remaining between time and ensemble averaged MSD in the latter strong (but finite) aging case is shown in Fig. 7. This difference decreases with growing aging time. From expansion of the prefactor Λ_α in Eq. (34) it follows via comparison with expression (26) that the difference between the ensemble and time averaged MSDs,

$$\langle x^2(t) \rangle_a - \left\langle \overline{\delta_a^2(\Delta)} \right\rangle \sim \frac{\alpha(\alpha-1)(\alpha-2)K_\alpha^*}{6k} \frac{t^2}{t_a^{3-\alpha}} \ll \langle x^2(t) \rangle_a \tag{35}$$

valid for $t_a \gg t \gg \Delta$, decays to zero rapidly with growing t_a. We also see that for $0 < \alpha < 1$ the ensemble averaged MSD is larger than the time averaged MSD, while the opposite is true for $1 < \alpha < 2$. In Fig. 7 we also demonstrate the convergence of ensemble and time averaged MSDs in the limit $\Delta \to t$.

IV. FIRST PASSAGE TIME DENSITY

Apart from the MSD the first passage behavior is a signature quantity of a stochastic process. We here study how aging changes the first passage statistic of SBM in the semi-infinite domain. The probability density function (PDF) of first passage is found by solving the SBM diffusion equation

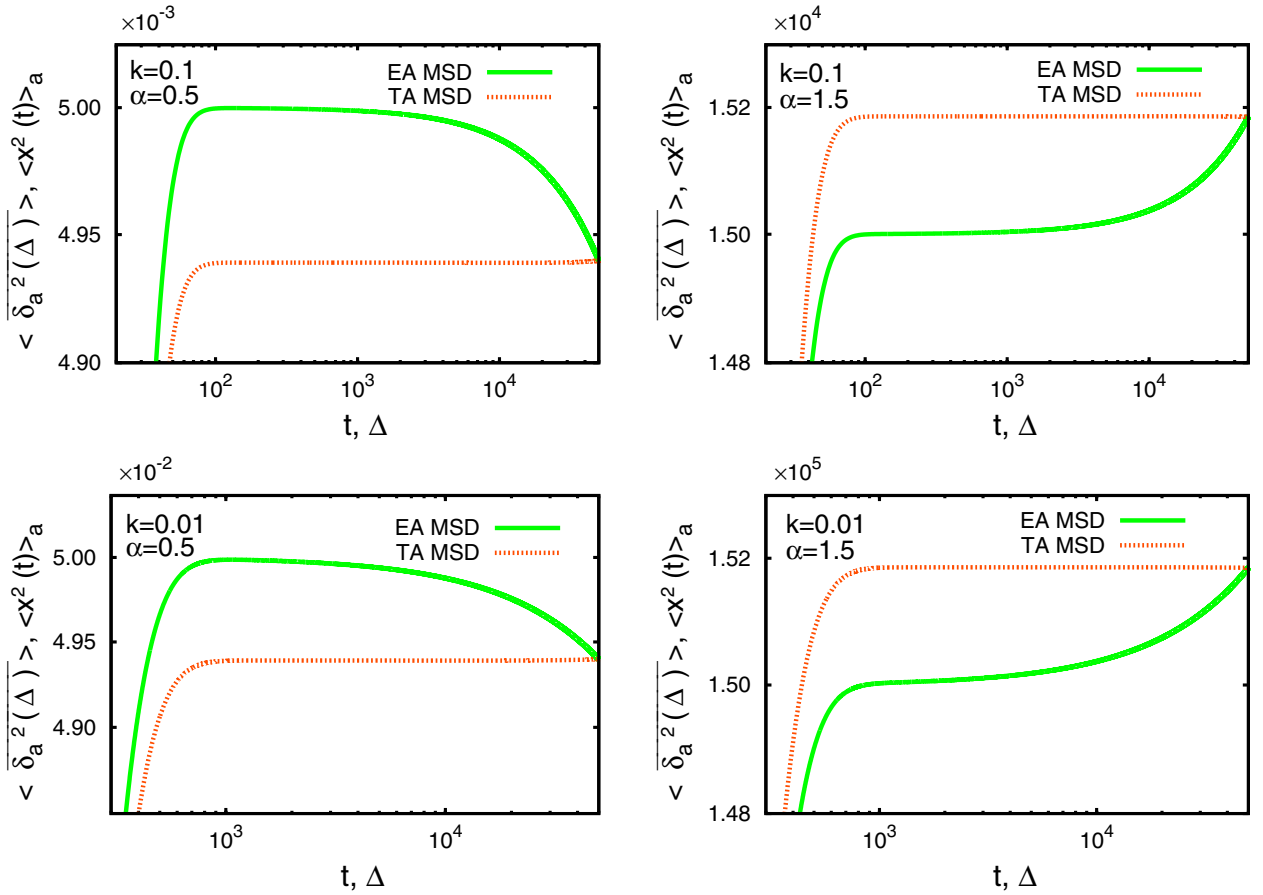

FIG. 7. (Color online) Full behavior of aging confined SBM for $t_a = 10^6$ with $\alpha = 1/2$ (left) and $\alpha = 3/2$ (right), demonstrating the convergence of the time averaged MSD to the ensemble averaged MSD in the limit $\Delta \to t$, shown for two different potential strengths, as indicated in the panels. The observation time is $t = 5 \times 10^4$. In accordance with result (35) the difference between ensemble and time averaged MSDs vanishes for growing aging time.

with the time dependent coefficient $\mathscr{K}(t)$,

$$\frac{\partial}{\partial t}P(x,t) = \mathscr{K}(t)\frac{\partial^2}{\partial x^2}P(x,t), \tag{36}$$

however, with the aged initial condition

$$P_0(x,t_a) = \frac{1}{\sqrt{4\pi K_\alpha^* t_a^\alpha}} e^{-x^2/(4K_\alpha^* t_a^\alpha)}. \tag{37}$$

This aged initial condition emerges from a $\delta(x)$ peak for a system initialized some aging time t_a before. In this setup t measures the time span from the aged initial condition (37). To obtain the first passage PDF for the semi-infinite domain we solve the SBM diffusion equation (36) for unconfined motion with the aged initial condition (37) and then use the method of images. For the PDF of the aged process we obtain

$$P(x,t) = \frac{1}{\sqrt{4\pi K_\alpha^* \left(t_a^\alpha + t^\alpha\right)}} e^{-x^2/4K_\alpha^*(t_a^\alpha + t^\alpha)}. \tag{38}$$

In the presence of an absorbing boundary at the origin, the survival probability for a process initiated originally in $x_0 > 0$ is therefore given by

$$\mathscr{S}(t) = \int_0^\infty [P(x - x_0,t) - P(x + x_0,t)]\, dx. \tag{39}$$

Substituting the aged PDF (37) into this expression yields

$$\mathscr{S}(t) = \mathrm{erf}\left(\frac{x_0}{\sqrt{4K_\alpha^*\left(t_a^\alpha + t^\alpha\right)}}\right) \tag{40}$$

in terms of the error function. The first passage PDF follows from the relation $\wp(t) = -d\mathscr{S}(t)/dt$,

$$\wp(t) = \frac{\alpha x_0 t^{\alpha-1}}{\sqrt{4\pi K_\alpha^* \left(t_a^\alpha + t^\alpha\right)^3}} \exp\left(-\frac{x_0^2}{4K_\alpha^*\left(t_a^\alpha + t^\alpha\right)}\right). \tag{41}$$

For $\alpha = 1$ (Brownian motion) and in the absence of aging ($t_a = 0$) we recover the well known Lévy-Smirnov distribution. Result (41) exhibits a crossover relative to the aging time,

$$\wp \simeq \frac{\alpha x_0}{\sqrt{4\pi K_\alpha^*}} \times \begin{cases} t_a^{-3\alpha/2} t^{\alpha-1}, & t_a \gg t, \left(x_0^2/[4K_\alpha^*]\right)^{1/\alpha}, \\ t^{-1-\alpha/2}, & t \gg t_a, \left(x_0^2/[4K_\alpha^*]\right)^{1/\alpha}. \end{cases} \tag{42}$$

In the strong aging limit the scaling exponent is $-(1-\alpha)$, and we observe the explicit presence of the aging time t_a with exponent α. For weak aging, the scaling exponent of t is $-(1+\alpha/2)$, as known from subdiffusive CTRW processes. However, the detailed crossover behavior is different, compare

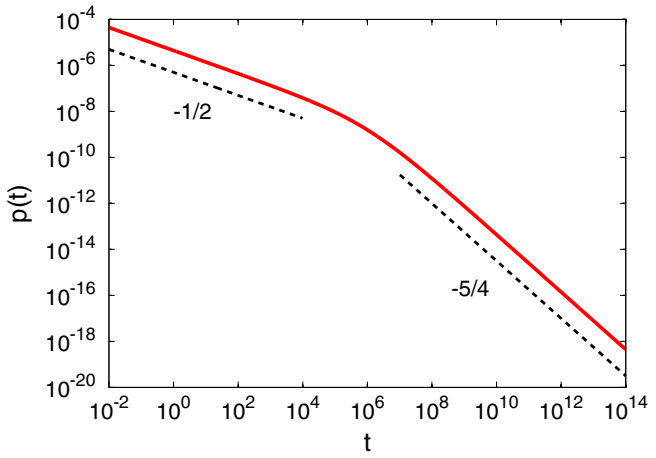

FIG. 8. (Color online) First passage time density $\wp(t)$ for $\alpha = 1/2$, with $x_0 = 1$, and aging time $t_a = 10^6$. As shown by the dashed line, the crossover between the aging dominated slope $-1/2$ to the slope $-5/4$ is distinct.

Ref. [48]. We also note that for fractional Brownian motion the anomalous diffusion exponent α enters oppositely [30,49]. Figure 8 shows the crossover of the first passage density for aging SBM.

V. CONCLUSIONS

SBM is possibly the simplest anomalous diffusion model, and it is therefore widely used in literature. Despite its apparent simplicity SBM exhibits weak ergodicity breaking in the sense that we observe a distinct disparity between the ensemble and time averaged MSDs of this process [26,27,31,32]. It is therefore a natural question to explore the aging effects of SBM, i.e., the explicit dependence of physical observables on the time span t_a between the original system preparation and start of the recording of the particle motion. We here showed how the ensemble and time averaged MSDs depend on t_a for both the unconfined and confined cases.

For unconfined aging SBM we obtained the exact dependence on the aging time t_a and observed a striking similarity to both subdiffusive CTRW with scale-free waiting time distributions and heterogeneous diffusion processes with power-law position dependence of the diffusivity. In particular, for short lag times the time averaged MSD factorizes into the nonaged expression and the aging depression Λ_α, which indeed has the same functional form as for the subdiffusive CTRW and the heterogeneous diffusion process. In the limit of strong aging, we also showed that ergodicity is seemingly restored and the disparity between ensemble and time averages becomes increasingly marginal. However, it should be stressed that due to its nonstationary nature the system still explicitly depends on the aging time t_a even in the limit when t_a tends to infinity.

Confined SBM, in contrast, is qualitatively a quite unique process. In absence of aging, due to the time dependence of the diffusivity $\mathscr{K}(t)$, there is no thermal plateau for the ensemble averaged MSD. Instead this quantity is continuously decaying (subdiffusion) or increasing (superdiffusion). As shown here the functional behavior of confined *aging* SBM is remarkably rich. Concurrently, the time averaged MSD exhibits an intermediate plateau. In the presence of aging we observe a deviation from the nonaged power-law behavior of the ensemble averaged MSD at longer times and a universal convergence to a plateau value. For strong aging we again observe the convergence of ensemble and time averaged MSDs. We note that the behavior of confined CTRW is opposite: The time averaged MSD exhibits a power-law growth with exponent $1 - \alpha$, while the ensemble averaged MSD converges to the thermal plateau value [33].

In addition to these quantities we considered the first passage time density in the semi-infinite domain. In contrast to the nonaging fractional Brownian motion we found a crossover between two characteristic scaling laws depending on the competition between aging and process time t_a and t.

When using SBM as a stochastic model cognizance should be taken of the fact that it is a highly nonstationary process. The time dependence of its diffusivity corresponds to a time dependent temperature (noise strength), and is therefore physically meaningless as description for a system coupled to a thermostat. There exist, however, cases in which SBM may turn out to be a physically meaningful approach. For instance, it was demonstrated that SBM provides a useful mean field description for the motion of a tagged particle in a granular gas with a subunity restitution coefficient in the homogeneous cooling phase [50].

A number of aging features are quite similar between subdiffusive CTRWs [36], heterogeneous diffusion processes [37], and aging SBM, as shown here. While fractional Brownian motion is ergodic, transient deviations from ergodicity and transient aging occur under confinement [17,51]. To reliably distinguish these models from another, it is therefore imperative to employ other diagnostic stochastic quantities with characteristic behaviors for the respective processes [27,52,53].

ACKNOWLEDGMENTS

A.V.C. acknowdges the IMU Berlin Einstein Foundation for financial support. R.M. acknowledges the Academy of Finland (Suomen Akatemia) for funding within the Finland Distinguished Professor (FiDiPro) scheme.

[1] L. F. Richardson, Proc. R. Soc. London Ser. A **110**, 709 (1926).
[2] H. Freundlich and D. Krüger, Trans. Faraday Soc. **31**, 906 (1935).
[3] J.-P. Bouchaud and A. Georges, Phys. Rep. **195**, 127 (1990).
[4] R. Metzler and J. Klafter, Phys. Rep. **339**, 1 (2000).
[5] H. Scher and E. W. Montroll, Phys. Rev. B **12**, 2455 (1975).
[6] M. Schubert, E. Preis, J. C. Blakesley, P. Pingel, U. Scherf, and D. Neher, Phys. Rev. B **87**, 024203 (2013).
[7] M. Dogan, R. L. Van Dam, G. C. Bohling, and J. J. Butler, Jr., Geophys. Rev. Lett. **38**, L06405 (2011); J. W. Kirchner, X. Feng, and C. Neal, Nature (London) **403**, 524 (2000); H. Scher, G. Margolin, R. Metzler, J. Klafter, and B. Berkowitz, Geophys. Res. Lett. **29**, 1061 (2002).

[8] E. R. Weeks, J. C. Crocker, A. C. Levitt, A. Schofield, and D. A. Weitz, Science **287**, 627 (2000); J. Mattsson, H. M. Wyss, A. Fernandez-Nieves, K. Miyazaki, Z. Hu, D. R. Reichman, and D. A. Weitz, Nature (London) **462**, 83 (2009).

[9] T. H. Solomon, E. R. Weeks, and H. L. Swinney, Phys. Rev. Lett. **71**, 3975 (1993); E. R. Weeks and H. L. Swinney, Phys. Rev. E **57**, 4915 (1998).

[10] F. Höfling and T. Franosch, Rep. Progr. Phys. **76**, 046602 (2013).

[11] M. J. Saxton, Biophys. J. **103**, 2411 (2012); **72**, 1744 (1997).

[12] J.-H. Jeon, V. Tejedor, S. Burov, E. Barkai, C. Selhuber-Unkel, K. Berg-Sørensen, L. Oddershede, and R. Metzler, Phys. Rev. Lett. **106**, 048103 (2011).

[13] S. M. A. Tabei, S. Burov, H. Y. Kim, A. Kuznetsov, T. Huynh, J. Jureller, L. H. Philipson, A. R. Dinner, and N. F. Scherer, Proc. Natl. Acad. Sci. USA **110**, 4911 (2013); D. Robert, T.-H. Nguyen, F. Gallet, and C. Wilhelm, PLoS ONE **5**, e10046 (2010).

[14] I. Golding and E. C. Cox, Phys. Rev. Lett. **96**, 098102 (2006); S. C. Weber, A. J. Spakowitz, and J. A. Theriot, *ibid.* **104**, 238102 (2010).

[15] K. Burnecki, E. Kepten, J. Janczura, I. Bronshtein, Y. Garini, and A. Weron, Biophys. J. **103**, 1839 (2012); I. Bronstein, Y. Israel, E. Kepten, S. Mai, Y. Shav-Tal, E. Barkai, and Y. Garini, Phys. Rev. Lett. **103**, 018102 (2009).

[16] W. Pan, L. Filobelo, N. D. Q. Pham, O. Galkin, V. V. Uzunova, and P. G. Vekilov, Phys. Rev. Lett. **102**, 058101 (2009); J. Szymanski and M. Weiss, *ibid.* **103**, 038102 (2009); G. Guigas, C. Kalla, and M. Weiss, Biophys. J. **93**, 316 (2007).

[17] J.-H. Jeon, N. Leijnse, L. B. Oddershede, and R. Metzler, New J. Phys. **15**, 045011 (2013).

[18] E. Yamamoto, T. Akimoto, M. Yasui, and K. Yasuoka, Sci. Rep. **4**, 4720 (2014); G. R. Kneller, K. Baczynski, and M. Pasienkewicz-Gierula, J. Chem. Phys. **135**, 141105 (2011); J.-H. Jeon, H. Martinez-Seara Monne, M. Javanainen, and R. Metzler, Phys. Rev. Lett. **109**, 188103 (2012).

[19] E. W. Montroll and G. H. Weiss, J. Math. Phys. **10**, 753 (1969).

[20] J. Klafter, A. Blumen, and M. F. Shlesinger, Phys. Rev. A **35**, 3081 (1987).

[21] B. B. Mandelbrot and J. W. van Ness, SIAM Rev. **10**, 422 (1968); A. N. Kolmogorov, Dokl. Acad. Sci. USSR **26**, 115 (1940).

[22] I. Goychuk, Phys. Rev. E **80**, 046125 (2009); Adv. Chem. Phys. **150**, 187 (2012); E. Lutz, Phys. Rev. E **64**, 051106 (2001); G. Kneller, J. Chem. Phys. **141**, 041105 (2014); P. Hänggi, Z. Phys. B **31**, 407 (1978); P. Hanggi and F. Mojtabai, Phys. Rev. A **26**, 1168(R) (1982); S. C. Kou, Ann. Appl. Stat. **2**, 501 (2008).

[23] S. Havlin and D. Ben-Avraham, Adv. Phys. **51**, 187 (2002); Y. Meroz, I. M. Sokolov, and J. Klafter, Phys. Rev. E **81**, 010101(R) (2010); M. Spanner, F. Höfling, G. E. Schröder-Turk, K. Mecke, and T. Franosch, J. Phys. Condens. Matter **23**, 234120 (2011).

[24] A. Klemm, H.-P. Müller, and R. Kimmich, Phys. Rev. E **55**, 4413 (1997); A. Klemm, R. Metzler, and R. Kimmich, *ibid.* **65**, 021112 (2002).

[25] A. G. Cherstvy, A. V. Chechkin, and R. Metzler, New J. Phys. **15**, 083039 (2013); Soft Matter **10**, 1591 (2014); A. G. Cherstvy and R. Metzler, Phys. Rev. E **90**, 012134 (2014); Phys. Chem. Chem. Phys. **15**, 20220 (2013); P. Massignan, C. Manzo, J. A. Torreno-Pina, M. F. García-Parajo, M. Lewenstein, and G. J. Lapeyre, Jr., Phys. Rev. Lett. **112**, 150603 (2014).

[26] A. Fuliński, J. Chem. Phys. **138**, 021101 (2013); Phys. Rev. E **83**, 061140 (2011).

[27] R. Metzler, J.-H. Jeon, A. G. Cherstvy, and E. Barkai, Phys. Chem. Chem. Phys. **16**, 24128 (2014).

[28] G. K. Batchelor, Math. Proc. Cambridge Philos. Soc. **48**, 345 (1952).

[29] M. J. Saxton, Biophys. J. **81**, 2226 (2001); T. J. Feder, I. Brust-Mascher, J. P. Slattery, B. Baird, and W. W. Webb, *ibid.* **70**, 2767 (1996); N. Periasmy and A. S. Verkman, *ibid.* **75**, 557 (1998); M. Weiss, M. Elsner, F. Kartberg, and T. Nilsson, *ibid.* **87**, 3518 (2004); J. Wu and K. M. Berland, *ibid.* **95**, 2049 (2008).

[30] S. C. Lim and S. V. Muniandy, Phys. Rev. E **66**, 021114 (2002).

[31] F. Thiel and I. M. Sokolov, Phys. Rev. E **89**, 012115 (2014).

[32] J.-H. Jeon, A. V. Chechkin, and R. Metzler, Phys. Chem. Chem. Phys. **16**, 15811 (2014).

[33] S. Burov, R. Metzler, and E. Barkai, Proc. Natl. Acad. Sci. USA **107**, 13228 (2010).

[34] E.-J. Donth, *The Glass Transition* (Springer, Berlin, 2001); W. Götze, *Complex Dynamics of Glass-Forming Liquids* (Oxford University Press, Oxford, UK, 2009).

[35] E. Barkai, Phys. Rev. Lett. **90**, 104101 (2003); E. Barkai and Y. C. Cheng, J. Chem. Phys. **118**, 6167 (2003).

[36] J. H. P. Schulz, E. Barkai, and R. Metzler, Phys. Rev. Lett. **110**, 020602 (2013); Phys. Rev. X **4**, 011028 (2014).

[37] A. G. Cherstvy, A. V. Chechkin, and R. Metzler, J. Phys. A **47**, 485002 (2014).

[38] W. E. Moerner and M. Orrit, Science **283**, 1670 (1999).

[39] M. J. Saxton and K. Jacobsen, Annu. Rev. Biophys. Biomol. Struct. **26**, 373 (1997).

[40] C. Bräuchle, D. C. Lamb, and J. Michaelis, *Single Particle Tracking and Single Molecule Energy Transfer* (Wiley-VCH, Weinheim, Germany, 2012).

[41] X. S. Xie, P. J. Choi, G.-W. Li, N. K. Lee, and G. Lia, Annu. Rev. Biophys. **37**, 417 (2008).

[42] J.-P. Bouchaud, J. Phys. (Paris) I **2**, 1705 (1992); C. Monthus and J.-P. Bouchaud, J. Phys. A **29**, 3847 (1996).

[43] E. Barkai, Y. Garini, and R. Metzler, Phys. Today **65**(8), 29 (2012).

[44] Y. He, S. Burov, R. Metzler, and E. Barkai, Phys. Rev. Lett. **101**, 058101 (2008).

[45] M. A. Taylor, J. Janousek, V. Daria, J. Knittel, B. Hage, H.-A. Bachor, and W. P. Bowen, Nat. Phot. **7**, 229 (2013).

[46] M. Abramowitz and I. A. Stegun, *Handbook of Mathematical Functions* (Dover, New York, 1965).

[47] A. B. Prudnikov and Yu. A. Brychkov, *Integrals and Series* (Gordon and Breach, New York, 1986), Vol. 3.

[48] H. Krüsemann, A. Godec, and R. Metzler, Phys. Rev. E **89**, 040101(R) (2014).

[49] J.-H. Jeon, A. V. Chechkin, and R. Metzler, Europhys. Lett. **94**, 20008 (2011).

[50] A. Bodrova, A. V. Chechkin, A. G. Cherstvy, and R. Metzler, arXiv:1501.04173.

[51] J. Kursawe, J. Schulz, and R. Metzler, Phys. Rev. E **88**, 062124 (2013); J.-H. Jeon and R. Metzler, *ibid.* **85**, 021147 (2012).

[52] V. Tejedor, O. Benichou, R. Voituriez, R. Jungmann, F. Simmel, C. Selhuber-Unkel, L. Oddershede, and R. Metzler, Biophys. J. **98**, 1364 (2010).

[53] M. Magdziarz, A. Weron, K. Burnecki, and J. Klafter, Phys. Rev. Lett. **103**, 180602 (2009).